ORGANIC LETTERS

2006
Vol. 8, No. 21
4951−4954

Photoinduced Cytotoxicity and Thioadduct Formation by a Prodigiosin Analogue

John T. Tomlinson,[†] Gyungse Park,[†] Jacob A. Misenheimer,[†] Gregory L. Kucera,[‡] Kevin Hesp,[§] and Richard A. Manderville*,[§]

Department of Chemistry, Wake Forest University, Winston-Salem, North Carolina 27109-7486, Section of Hematology−Oncology, Wake Forest University School of Medicine, Winston-Salem, North Carolina 27157, Department of Chemistry, University of Guelph, Guelph, Ontario, Canada N1G 2W1

rmanderv@uoguelph.ca

Received August 11, 2006

ABSTRACT

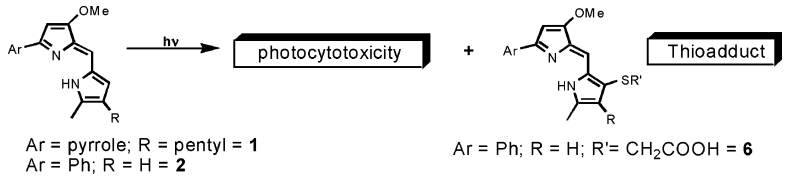

The prodigiosin alkaloid 1 and the synthetic analogue 2 show photoinduced cytotoxicity against HL-60 cancer cells. Photoirradiation of 1 and 2 causes photofading, photooxidation, and thioadduct formation. These results provide a model for the redox properties of prodigiosins that play a role in their biological activity and provide a new way to functionalize their pyrromethene entity with water-soluble thiol groups.

The prodigiosins are a family of red pigments produced by certain strains of *Serratia marcesens*. These alkaloids contain a characteristic pyrrolylpyrromethene skeleton with a **B**-ring methoxy group.[1] Prodigiosin (**1**, Figure 1), the parent member

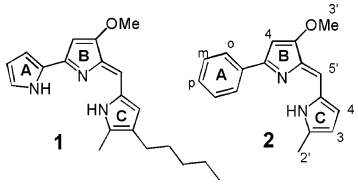

Figure 1. Prodigiosin (**1**) and synthetic analogue **2**.

of this family, has been noted for immunosuppressive activity[2] and has been identified as a mediator of apoptosis in dozens of human cancer cells with little effect on nonmalignant cells.[3]

The therapeutic potential of prodigiosins has stimulated research into their mechanism of action. Structure−activity relationships establish that a nitrogen-containing heterocyclic **A**-ring[4] and a methoxy group[5] at the 3-position of the **B**-ring are important for cytotoxic potency. In addition to proposed

[†] Wake Forest University.
[‡] Wake Forest University School of Medicine.
[§] University of Guelph.

10.1021/ol061998r CCC: $33.50
Published on Web 09/15/2006

(1) For reviews, see: (a) Manderville, R. A. *Curr. Med. Chem.: Anti−Cancer Agents* **2001**, *1*, 195−218. (b) Fürstner, A. *Angew. Chem., Int. Ed.* **2003**, *42*, 3582−3603.

(2) (a) Magae, J.; Yamashita, M.; Nagai, K. *Ann. N.Y. Acad. Sci.* **1993**, *685*, 339−340. (b) Mortellaro, A.; Songia, S.; Gnocchi, P.; Ferrari, M.; Fornasiero, C.; D'Alessio, R.; Isetta, A.; Colotta, F.; Golay, J. *J. Immunol.* **1999**, *162*, 7102−7109. (c) Stepkowski, S. M.; Erwin-Cohen, R. A.; Behbod, F.; Wang, M. E.; Qu, X.; Tejpal, N.; Nagy, Z. S.; Kahan, B. D.; Kirken, R. A. *Blood* **2002**, *99*, 680−689.

(3) (a) Yamamoto, C.; Takemoto, H.; Kuno, K.; Yamamoto, D.; Tsubura, A.; Kamata, K.; Hirata, H.; Yamamoto, K.; Kano, H.; Seki, T.; Inoue, K. *Hepatology* **1999**, *30*, 894−902. (b) Baldino, C. M.; Parr, J.; Wilson, C. J.; Ng, S.-C.; Yohannes, D.; Wasserman, H. H. *Bioorg. Med. Chem. Lett.* **2006**, *16*, 701−704.

(4) D'Alessio, R.; Bargiotti, A.; Carlini, O.; Colotta, F.; Ferrari, M.; Gnocchi, P.; Isetta, A.; Mongelli, N.; Motta, P.; Rossi, A.; Rossi, M.; Tibolla, M.; Vanotti, E. *J. Med. Chem.* **2000**, *43*, 2557−2565.

(5) Boger, D. L.; Patel, M. *J. Org. Chem.* **1988**, *53*, 1405−1415.

H^+/Cl^- symport activities,[6,7] prodigiosins also bind DNA effectively[8] and facilitate oxidative DNA cleavage in the presence of copper^{2+} (Cu(II)).[9] The nuclease activity is thought to occur via π-radical cation formation at the electron-rich pyrrolylpyrromethene entity. This event could be stimulated by the interaction of Cu(II) to yield Cu(I), which is known to foster reductive activation of molecular oxygen (O_2) leading to the formation of a superoxide radical anion ($O_2^{\bullet-}$) and hence hydrogen peroxide (H_2O_2). The interaction of H_2O_2 with a Cu-bound prodigiosin species[10] is thought to initiate DNA cleavage. Structure−activity relationships demonstrate that replacement of the individual metal-coordinating pyrrole rings by other weaker Cu(II)-ligating arenes results in marked loss of nuclease activity and cytotoxicity.[11]

Although coordination of **1** to a redox-active metal cation represents one way of triggering oxidation of the natural alkaloid, Roth noted that prodigiosins also possess photosensitizing activity.[12] Here, exposure of colorless mutant *Sarcina lutea* cells to prodigiosin and visible light led to cell death in an O_2-dependent process. Thus, we speculated that **1** would undergo photooxidation to reductively activate O_2 and yield prodigiosin-derived π-radical cations that may act to facilitate tumor destruction. Presently, we report on our initial findings regarding photoinduced cytotoxicity of prodigiosin (**1**) and the synthetic analogue **2** (Figure 1) against HL-60 leukemia cancer cells. Our results provide new insights into the redox properties of prodigiosin analogues and afford design ideas for their development as photoactivatable anticancer agents.

Although prodigiosin (**1**) exhibited an increase in cytotoxicity when exposed to visible light, the pigment was too active in the absence of light. Our initial strategy to inhibit dark cytotoxicity was to replace the **A**-pyrrole of **1** with an alternative, nonmetal-coordinating arene.[4,12] Scheme 1 shows the synthesis of the phenyl analogue **2** that was prepared using the strategies outlined by D'Alessio and Rossi[13] (see Supporting Information for details).

The ability of **1** and **2** to inhibit cancer cell growth in the absence and presence of visible light was then determined

Scheme 1. Synthesis of Prodigiosin Analogue **2**

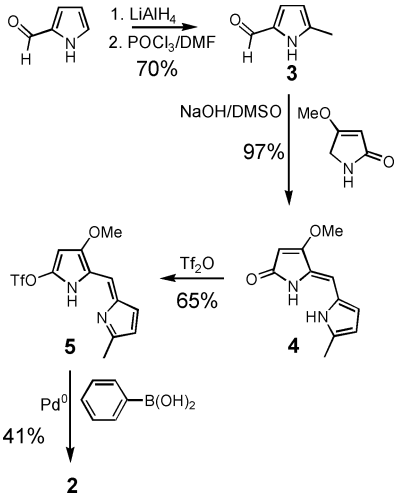

using human promyelocytic leukemia (HL-60) cells. These cells have been utilized previously by our research group to determine structure−activity relationships for the prodigiosins.[10,12b] Prodigiosin (**1**) exhibited an IC_{50} value of ~6.6 μM following 4 h of drug exposure. Under analogous conditions, the synthetic derivative **2** failed to inhibit colony formation at 25 μM, which was the maximum drug concentration examined (IC_{50} (dark), see Table 1). The photocytotoxicity of **1** and **2** was then determined by exposing HL-60 cells to drug and visible light (λ > 495 nm) for 30 min followed by incubation for an additional 3.5 h in the absence of light. Cells exposed to 30 min of light in the absence of drug showed no inhibition of colony formation. As shown in Table 1, prodigiosin **1** was more active with irradiation (IC_{50} (dark) vs IC_{50} (light)), as was the derivative **2** (IC_{50} (light) = 16.2 μM). These results demonstrated that prodigiosin-based pigments can serve as photoactivatable anticancer agents.

Table 1. Inhibition of HL-60 Cell Growth by Prodigiosins[a]

compound	IC_{50} (dark)	IC_{50} (light)[c]
1	6.6 ± 0.1	2.5 ± 0.2
2	>25[b]	16.2 ± 0.2

[a] Inhibition of colony formation was assessed using the soft agar clonogenic survival assay as described in the Supporting Information. Values in micromolar are expressed as the mean of three determinations. [b] No inhibition at 25 μM drug. [c] Inhibition following 4 h exposure to the drug in the presence of 30 min exposure to visible light (>495 nm).

To determine how **1** and **2** may stimulate photocytotoxicity, their photoreactions in buffered water were studied using absorption spectroscopy and LC-MS for product analysis. Figure 2 shows the absorption spectra of **1** (7 μM) and **2** (18 μM) before and after different irradiation times. For **1** (Figure 2A), the absorption maxima at 538 nm decreased together with the shoulder at 487 nm ($\epsilon_{487}/\epsilon_{538}$ = 0.74) by 38% following 30 min. For **2** (Figure 2B), the

(6) Sessler, J. L.; Eller, L. R.; Cho, W.-S.; Nicolaou, S.; Aguilar, A.; Lee, J. T.; Lynch, V. M.; Magda, D. J. *Angew. Chem., Int. Ed.* **2005**, *44*, 5989−5992.

(7) (a) Sato, T.; Konno, H.; Tanaka, Y.; Kataoka, T.; Nagai, K.; Wasserman, H.; Ohkuma, S. *J. Biol. Chem.* **1998**, *273*, 21455−21462. (b) Gale, P. A.; Light, M. E.; McNally, B.; Navakhun, K.; Sliwinski, K. E.; Smith, B. D. *Chem. Commun.* **2005**, 3773−3775.

(8) (a) Melvin, M. S.; Ferguson, D. C.; Lindquist, N.; Manderville, R. A. *J. Org. Chem.* **1999**, *64*, 6861−6869. (b) Montaner, B.; Castillo-Ávila, W.; Martinell, M.; Öllinger, R.; Aymami, J.; Giralt, E.; Pérez-Tomás, R. *Toxicol. Sci.* **2005**, *85*, 870−879.

(9) (a) Melvin, M. S.; Tomlinson, J. T.; Saluta, G. R.; Kucera, G. L.; Lindquist, N.; Manderville, R. A. *J. Am. Chem. Soc.* **2000**, *122*, 6333−6334. (b) Melvin, M. S.; Wooton, K E.; Rich, C. C.; Saluta, G. R.; Kucera, G. L.; Lindquist, N.; Manderville, R. A. *J. Inorg. Biochem.* **2001**, *87*, 129−135.

(10) Park, G.; Tomlinson, J. T.; Melvin, M. S.; Wright, M. W.; Day, C. S.; Manderville, R. A. *Org. Lett.* **2003**, *5*, 113−116.

(11) (a) Fürstner, A.; Grabowski, E. J. *ChemBioChem* **2001**, *9*, 706−709. (b) Melvin, M. S.; Tomlinson, J. T.; Park, G.; Day, C. S.; Saluta, G. R.; Kucera, G. L.; Manderville, R. A. *Chem. Res. Toxicol.* **2002**, *15*, 734−741.

(12) Roth, M. M. *Photochem. Photobiol.* **1967**, *6*, 923−926.

(13) D'Alessio, R.; Rossi, A. *Synlett* **1996**, 513−514.

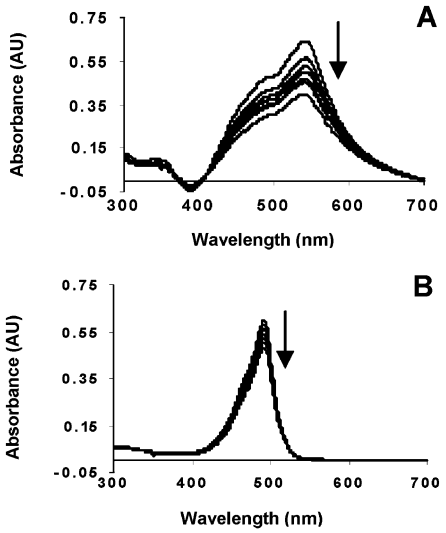

Figure 2. Absorption spectra of **1** (7 μM) (A) and **2** (18 μM) (B) in buffered water (MOPS, 10 mM, pH 7, 0.1 M NaCl) after different irradiation times: 0, 5, 10, 15, 20, 25, and 30 min.

absorption maxima at 490 nm also decreased, but only by 20% following 30 min of irradiation. These results demonstrated that **1** is more photoreactive than **2**, which is consistent with its superior photocytotoxicity (Table 1).

Certain dyes produce reactive oxygen species (ROS) that, in turn, attack the dye and result in photofading.[14] Pyrromethene (BODIPY) dyes[15] and pyrroles[16] are known to undergo photooxidation in the presence of O_2. Laser flash photolysis studies on BODIPY dyes show radical cation formation by photoinduced electron-transfer processes.[15] These dyes possess electrochemical oxidation potentials ~ 0.9 V (vs SCE),[15] which are 400 mV higher than the oxidation potential of **1**,[17] suggesting that **1** would be even more prone to photooxidation. Thus, the irradiated sample of **1** was examined by ES^+−MS to determine whether photoproducts were produced. As shown in Figure S1 (Supporting Information), two photoproducts (**a** and **b**) were generated with *m*/*z* 340, which is 16 mass units heavier than the parent **1** ($[M + H]^+ = 324$). Collision-induced dissociation of **b** yielded a species with *m*/*z* 323 for loss of 17 mass units (OH). Photoproduct **a** generated species with *m*/*z* 325 and 308 for losses of 15 (CH_3) and 17 (OH) mass units, respectively (Supporting Information, Figure S1); prodigiosin **1** shows a loss of 15 mass units (CH_3) from the **B**-ring methoxy group. These results suggested photooxidation of **1** leading to OH attachment, which correlates with our previous findings that Cu(II) complexation by **1** yields a complex with an OH group attached to the **C**-ring.[10] The analogue **2** did not show photoproducts following 30 min of irradiation (not shown). Replacement of the **A**-pyrrole ring of **1** with a phenyl group raises the electrochemical oxidation potential by ~240 mV,[17] and so **2** would be more resistant to photooxidation and hence photofading[14] (Supporting Information, Figure 2B).

Further experiments with **2** were carried out to determine whether irradiation triggers its attachment to a thiol nucleophile. For these studies, we utilized thioglycolic acid (TGA) that has been employed to trap indole electrophiles.[18] The synthetic derivative **2** is also more water-soluble than **1** and was available in our laboratory in sufficient quantities to carry out such a product analysis. For these experiments, 4.8 mM **2** in the presence of 48 mM TGA was irradiated in buffered water (0.5 M MES, pH 6.0, 0.1 M NaCl, total volume of 5 mL) for 30 min and then the mixture was incubated for 2 h at 37 °C. Reaction products were analyzed by ES^+−MS and isolated using semipreparative HPLC.

Figure 3 shows an overlay of the ^{1}H NMR spectra

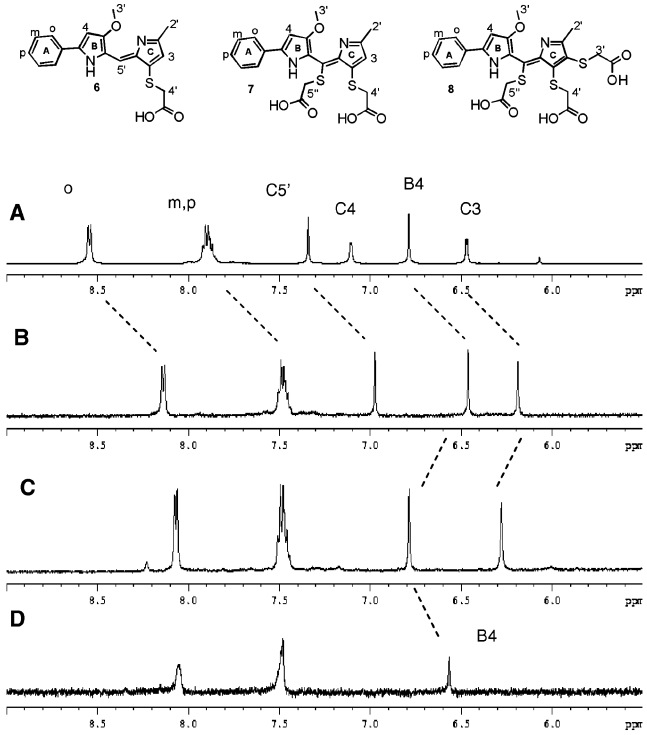

Figure 3. Aromatic region of the 500 MHz ^{1}H NMR spectra of (A) **2**; (B) **6**; (C) **7**; and (D) **8**, recorded in DMSO-d_6.

(aromatic region) of **2** and three TGA conjugates that were isolated from the photoreaction. The conjugates formed in a sequential fashion with the monoconjugate **6** forming first, followed by the $(TGA)_2$ conjugate **7** and finally the $(TGA)_3$ conjugate **8** with [**6**] > [**7**] > [**8**].[19] The conjugate **6** had an $[M + H]^+$ peak at *m*/*z* 355 and a UV−vis absorbance at

(14) Kanony, C.; Akerman, B.; Tuite, E. *J. Am. Chem. Soc*. **2001**, *123*, 7985−7995.
(15) Jones, G., II; Kumar, S.; Klueva, O.; Pacheco, D. *J. Phys. Chem. A* **2003**, *107*, 8429−8434.
(16) Lightner, D. A.; Crandall, D. C. *Tetrahedron Lett.* **1973**, 1799−1803.
(17) Melvin, M. S.; Calcutt, M. W.; Noftle, R. E.; Manderville, R. A. *Chem. Res. Toxicol.* **2002**, *15*, 742−748.
(18) Skordos, K. W.; Laycock, J. D.; Yost, G. S. *Chem. Res. Toxicol.* **1998**, *11*, 1326−1331.

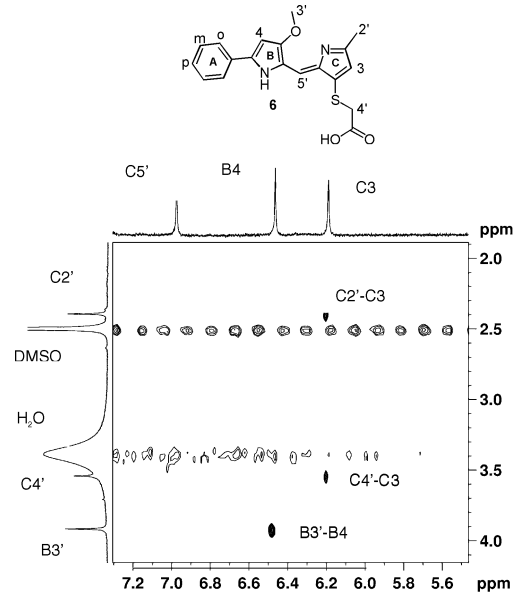

Figure 4. NOESY spectrum of **6** in DMSO-d_6 showing the B3′−B4, C4′−C3, and C2′−B4 cross-peaks.

λ_{max} 510 nm (diode array detector) that is red shifted by 20 nm compared to **2**. Its ^{1}H NMR spectrum in Figure 3B showed three singlets on the pyrromethene ring system suggesting TGA attachment to the **C**-ring of **2**. Unambiguous structural assignment of **6** was afforded by the NOESY spectrum shown in Figure 4; the B3′−B4, C4′−C3, and C2′−C3 cross-peaks confirmed C4 attachment by the first TGA. The $(TGA)_2$ conjugate **7** had an $[M + H]^+$ peak at *m*/*z* 445 and a UV−vis absorbance at λ_{max} 526 nm that is red-shifted by 16 nm compared to **6** and by 36 nm compared to **2**. For **7**, assignment of the B4 proton was achieved from observation of o−B4 and B3′−B4 cross-peaks in the NOESY spectrum (Supporting Information, Figure S2). The C3 proton assignment followed from HMQC and HMBC spectra (Supporting Information, Figure S3) in which the C2′ methyl protons at 2.3 ppm showed a long-range correlation (HMBC spectrum) with the C3 carbon at 113 ppm. The final $(TGA)_3$ conjugate **8** with the single proton on the pyrromethene moiety (Figure 3D) had an $[M + H]^+$ peak at *m*/*z* 535 and a UV−vis absorbance at λ_{max} 536 nm; its assignment was confirmed by its NOESY spectrum shown in Supporting Information Figure S4 that displayed o−B4 and B3′−B4 cross-peaks.

Photoinduced thioadduct formation by **2** demonstrates the existence of a reactive intermediate centered on the pyrromethene moiety. We propose the mechanism outlined in Scheme 2 for the production of **6**. The first step involves

Scheme 2. Proposed Mechanism for Production of **6**

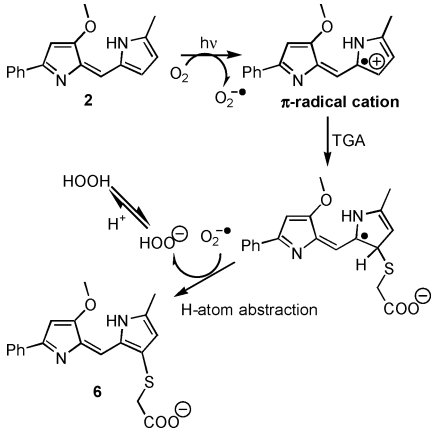

π-radical cation formation with reduction of O_2 producing $O_2^{\bullet-}$, as proposed for BODIPY dyes.[15] Attachment of TGA to the π-radical cation would yield a radical intermediate that requires H-atom abstraction, possibly by $O_2^{\bullet-}$, to yield **6**. The conjugate **6**, which is more electron rich than the parent **2**, undergoes further reactions to generate **7** and **8**. These results highlight the photoinduced redox properties of prodigiosins that may provide a model for biological activity. For example, Fürstner and co-workers reported that prodigiosins act as tyrosine phosphatase inhibitors and speculated that prodigiosin-derived electrophiles may target active site cysteine residues.[20] Our results give credence to this hypothesis and provide a new means of functionalizing the pyrromethene chromophore with water-soluble thiol groups. Compared to the parent pigments, such thioadducts may display superior biological properties.

In conclusion, we have demonstrated the photocytotoxicity of prodigiosins and have shown that the photoreaction generates thioadducts for the synthetic analogue **2**. The development of more potent prodigiosin-based photocytotoxic agents appears possible.

Acknowledgment. Acknowledgment is made to the Drug Synthesis & Chemistry Branch, Developmental Therapeutics Program, Division of Cancer Treatment and Diagnosis of the National Cancer Institute for the sample of prodigiosin.

Supporting Information Available: Experimental details and Figures S1−S4 described in the text. This material is available free of charge via the Internet at http://pubs.acs.org.

OL061998R

(19) Thioadducts **6**−**8** are depicted in the α-form, with an *E* double bond connecting the **B** and **C** rings, for convenience. Our NMR data do not differentiate between the α-form and the β-form used to depict **1** and **2** in Figure 1.

(20) Fürstner, A.; Reinecke, K.; Prinz, H.; Waldmann, H. *ChemBioChem* **2004**, *5*, 1575−1579.